

# Caging Effects on the Ground and Excited States of 2,2'-Bipyridine-3,3'-diol Embedded in Cyclodextrins

Osama K. Abou-Zied\* and Ashraf T. Al-Hinai

Department of Chemistry, Faculty of Science, Sultan Qaboos University, P.O. Box 36, Al-Khodh, Postal Code 123, Muscat, Sultanate of Oman

Received: March 15, 2006; In Final Form: April 24, 2006

The 2,2'-bipyridine-3,3'-diol (BP(OH)<sub>2</sub>) molecule shows unique spectroscopic features in water that may position it as a new biological probe. In an attempt to mimic biological environments, we explore in this paper the caging effects of cyclodextrins on the steady state spectra of BP(OH)<sub>2</sub>. The caging effects of  $\gamma$ -,  $\beta$ -, and 2,6-di-*O*-methyl- $\beta$ -cyclodextrins (CDs) on the ground and excited state properties of BP(OH)<sub>2</sub> in aqueous solutions are investigated by steady state absorption and fluorescence spectroscopy, and by ab initio calculations. The stoichiometry of the three complexes was found to be 1:1 and the binding constants were estimated from the absorption and fluorescence spectra. In the case of  $\gamma$ -CD, the large cavity size supports only small binding, whereas such binding increases in the cases of the smaller cavity sizes of  $\beta$ -CD and 2,6-di-*O*-methyl- $\beta$ -CD. Maximum binding was measured in the case of 2,6-di-*O*-methyl- $\beta$ -CD due to the increased hydrophobicity of the host cavity. The unique absorption features of BP(OH)<sub>2</sub> in water show a dramatic decrease in intensity due to caging effects. The decrease in intensity correlates very well with the extent of binding and hydrophobicity of the host molecules. Similar results were also obtained from the fluorescence spectra. The calculated structure of the BP(OH)<sub>2</sub>: $\beta$ -CD complex predicts that the inclusion of BP(OH)<sub>2</sub> is nearly axial and centered inside the  $\beta$ -CD cavity. The BP(OH)<sub>2</sub> molecule maintains its dienol moiety in the complex with no possible hydrogen bonding with the host interior H-atoms. The results are discussed in light of the possible use of BP(OH)<sub>2</sub> as a water sensor in biological systems.

## Introduction

The 2,2'-bipyridine-3,3'-diol (BP(OH)<sub>2</sub>) molecule (shown in Figure 1) is known to undergo an ultrafast excited state intramolecular double proton transfer (ESIDPT) in solution.<sup>1</sup> At room temperature, BP(OH)<sub>2</sub> absorbs in the region of 350 nm yet fluoresces strongly in the green. Quantum yields of fluorescence on the order of 0.2–0.4 were observed in different solvents at room temperature with lifetimes of a few nanoseconds.<sup>1–5</sup> Comparison of the absorption and emission properties of BP(OH)<sub>2</sub> with related systems possessing only one hydrogen bond reveals that the second hydroxyl group is essential to the observation of the strong green emission. This molecule is also planar in crystalline form<sup>6</sup> and is expected to retain its planarity in solutions of noninteracting solvents because of the two strong intramolecular hydrogen bonds. Electrooptical absorption and emission and calculated excited state dipole moments show that the dipole moments of the dienol (DE) and the diketo (DK) tautomers are negligible, whereas it is 4.0–4.9 D for the monoketo (MK) tautomer.<sup>7,8</sup> Several experimental<sup>9–13</sup> and theoretical<sup>14–17</sup> studies have characterized the ultrafast dynamics in photoexcited BP(OH)<sub>2</sub> and the double proton transfer was concluded to occur through both concerted and stepwise mechanisms.

We have recently proposed BP(OH)<sub>2</sub> as a model for natural base pairs to study tautomerization in duplex DNA.<sup>18</sup> Molecular dynamics simulations were performed for a dodecamer duplex DNA containing BP(OH)<sub>2</sub> as a model base pair in the center of the duplex. The results of the simulations indicate that BP(OH)<sub>2</sub>

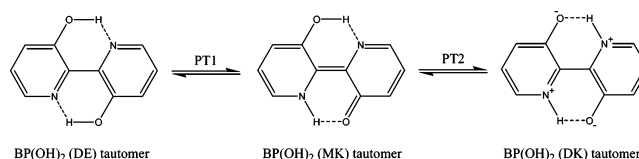


**Figure 1.** Tautomerization in BP(OH)<sub>2</sub> after single proton transfer (PT1) and double proton transfer (PT2).

can serve as a good mimic of a natural base pair with no major perturbation to the helical structure's stability. One of the two hydrogen bonds in BP(OH)<sub>2</sub> resides in the major groove of the duplex DNA, whereas the other one is situated in the minor groove. Similar biological environments were then tested by studying the steady state absorption and fluorescence spectra of BP(OH)<sub>2</sub> in solvents of varying polarity and hydrogen bonding capability, and in binary mixtures of 1,4-dioxane/water. Unique absorption due to water solvation was observed in the region of 400–450 nm. A large blue shift in the fluorescence band due to intermolecular hydrogen bonding was observed in polar, protic solvents. The shift increases with increasing solvent polarity. The geometry of BP(OH)<sub>2</sub> inside the DNA duplex and its unique spectroscopic characters in water suggest that this molecule can serve as a possible water sensor in DNA.

We extend the above study to include the caging effect on the steady state spectra of BP(OH)<sub>2</sub> aqueous solution. This caging effect can be induced in heterogeneous environments that are capable of providing nanopockets of desired polarity and viscosity. These environments can be attained by aqueous cyclodextrins (CDs) that quite often provide nanoenvironments very similar to biological environments. CDs are linked glucopyranose rings forming a doughnut shaped structure.<sup>19</sup> The

\* Corresponding author. Tel.: (+968) 2414-1468. Fax: (+968) 2414-1469. E-mail: abouzied@squ.edu.om.

number of glucose units and, consequently, the cavity diameter increases on going from  $\alpha$ -CD to  $\gamma$ -CD through  $\beta$ -CD.<sup>20</sup> CDs with different cavity diameters have been used advantageously to sequester guests on the basis of size. This property has been exploited to use CDs in drug delivery techniques. They are, thus, interesting nanovessels for appropriately sized molecules and the resulting supramolecules serve as excellent miniature models of enzyme–substrate complexes. The reduced polarity and the restricted space provided by the CD cavity markedly influence a number of photophysical and photochemical processes.<sup>21,22</sup> For example, Shizuka et al. have demonstrated that proton transfer reactions are affected by inclusion of the substrate molecules in CD cavities.<sup>23,24</sup> Their fluorescence studies have revealed that 2-naphthol forms 1:1 inclusion complexes with  $\alpha$ -,  $\beta$ - and  $\gamma$ -CDs with different association constants.

In the present paper, CDs are used to mimic the stacking effect of duplex DNA. In that aspect, the role played by the CD cavity in protecting the guest molecule against the approach of water molecules resembles the stacking inside DNA which tends to keep the base pairs away from water present in the major and minor grooves of the duplex. We show that the steady state absorption and fluorescence spectra of BP(OH)<sub>2</sub> are very sensitive to environmental changes due to the presence of CDs in solution. The present study focuses on the inclusion of BP(OH)<sub>2</sub> in the cavity of  $\beta$ -CD. We change the hydrophobic environment and the size of the cavity by carrying out the study in a substituted  $\beta$ -CD and in  $\gamma$ -CD. Finally, we present a calculated structure for the inclusion of BP(OH)<sub>2</sub> inside the  $\beta$ -CD cavity.

### Experimental and Theoretical Methods

BP(OH)<sub>2</sub> (98%) was obtained from Aldrich Chemical Co., Inc. and was used without further purification.  $\beta$ -CD ( $\geq 99\%$ ), 2,6-di-*O*-methyl- $\beta$ -CD (DM $\beta$ -CD) ( $\geq 98\%$ ) and  $\gamma$ -CD ( $\geq 98\%$ ) were purchased from Fluka and used as received. Millipore water was used in all the experiments. The concentration of BP(OH)<sub>2</sub> in solution was 10  $\mu$ M. Complexes of BP(OH)<sub>2</sub> with CDs were prepared and allowed to equilibrate for 12 h before taking the measurements. Absorption spectra were obtained with an HP 845x diode array spectrophotometer. Fluorescence spectra were recorded on a Shimadzu RF-5301 PC spectrofluorophotometer. In all the experiments, samples were contained in a 1 cm path length quartz cell and the measurements were performed at  $23 \pm 1$  °C through a carefully controlled lab temperature.

Geometry optimization of the BP(OH)<sub>2</sub>/ $\beta$ -CD complex was carried out using the GAMESS program<sup>25</sup> at the 3-21G level of calculations.

### Results and Discussion

**Steady State Absorption Spectra.** The steady state absorption spectra of BP(OH)<sub>2</sub> in aqueous solutions with varying concentrations of  $\gamma$ -CD,  $\beta$ -CD and DM $\beta$ -CD are shown in Figure 2 for the region from 270 to 470 nm. The peak at 344 nm represents the transition to the lowest <sup>1</sup>( $\pi,\pi^*$ ) state.<sup>1</sup> The double-peak absorption in the region of 400–450 nm is due to water solvation,<sup>18,26</sup> and was suggested to be due to the stabilization of the DK tautomer in the ground state.<sup>26,27</sup> The absorption spectra of BP(OH)<sub>2</sub> in water and in cyclohexane are shown in Figure 3 for comparison. In cyclohexane, there is no measurable absorbance in the region 400–450 nm, whereas in water the absorbance intensity in this region is high and gains its strength at the expense of that at 344 nm. Accordingly, the degree of encapsulation of the BP(OH)<sub>2</sub> molecule inside a given

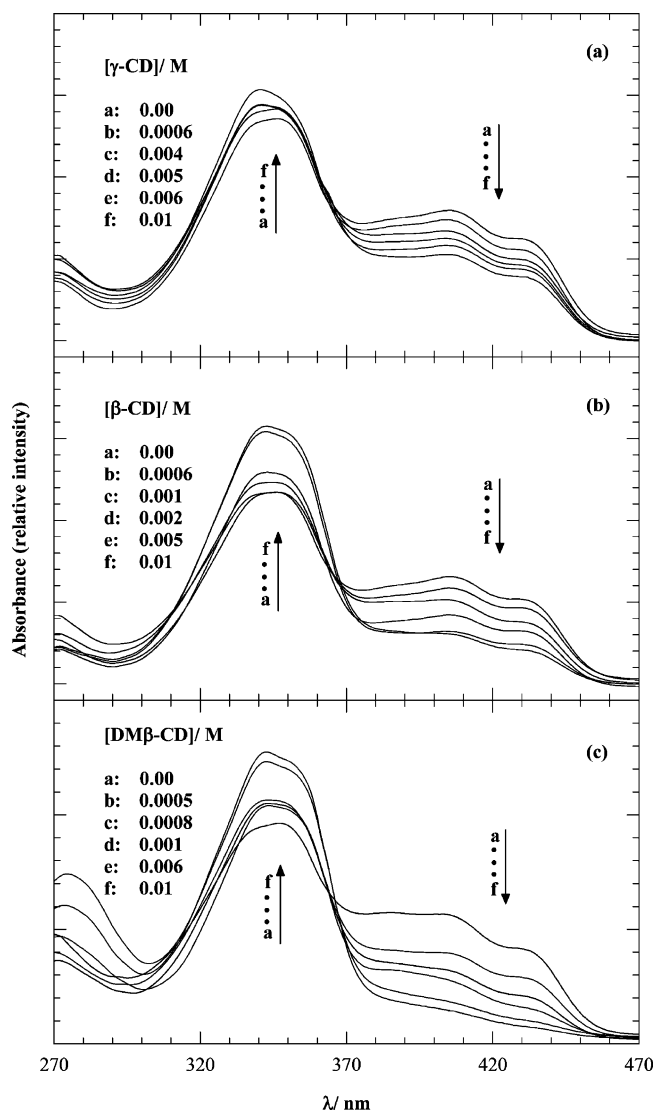


**Figure 2.** Absorption spectra of BP(OH)<sub>2</sub> in aqueous solutions with varying concentrations of (a)  $\gamma$ -CD, (b)  $\beta$ -CD and (c) DM $\beta$ -CD as indicated in each figure.

CD cavity can be correlated to the amount of the absorption change in the region of 400–450 nm (vide infra).

As the CD concentration increases, all the spectra in Figure 2 show a similar trend, which is an increase in the intensity of the peak at 344 nm with a concomitant decrease in the intensity of the two peaks in the region 400–450 nm. This trend is due to the caging effect of the CD cavity on the guest molecule. Upon complexation, the BP(OH)<sub>2</sub> molecule will experience shielding from the water molecules outside the CD cavity. Hence, the decrease in the absorbance intensity in the region 400–450 nm is a manifestation of how deep the BP(OH)<sub>2</sub> molecule is buried inside the CD cavity. In the case of  $\gamma$ -CD, this trend is somewhat small, indicating a small effect of complexation in protecting the BP(OH)<sub>2</sub> molecule from water due to the wide cavity size (an inner diameter of 0.95 nm<sup>20</sup>). On the other hand, the above trend is more pronounced in the case of BP(OH)<sub>2</sub>/ $\beta$ -CD, which indicates the deeper penetration of the guest molecule inside the narrower CD cavity (inner diameter 0.78 nm<sup>20</sup>). In the case of BP(OH)<sub>2</sub>/DM $\beta$ -CD, the effect of caging is even more dramatic than in the case of BP(OH)<sub>2</sub>/ $\beta$ -CD, as shown in Figure 2.

Both  $\beta$ -CD and DM $\beta$ -CD have the same cavity diameter, but the hydrogen-bonding ability of the alcoholic hydrogens in  $\beta$ -CD

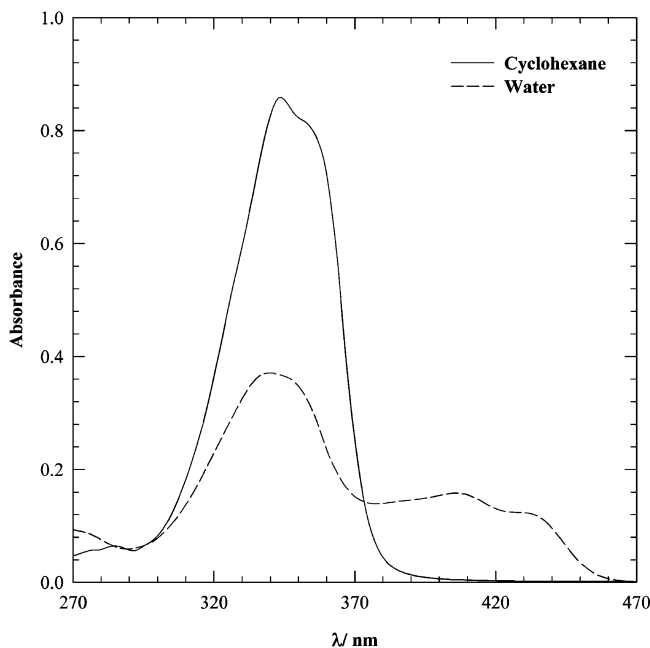


**Figure 3.** Absorption spectra of BP(OH)<sub>2</sub> in cyclohexane and water. Peaks at 409 and 435 nm are due to water solvation of the hydrogen bonding centers.

is low compared to that of DM $\beta$ -CD because, in the former, the secondary alcoholic -OH groups at the 2- and 3-positions of the adjacent glucopyranose rings are engaged in intramolecular hydrogen-bonding with each other. As a result,  $\beta$ -CD is less soluble in water than DM $\beta$ -CD. In the case of DM $\beta$ -CD, however, this intramolecular hydrogen-bonding is destroyed due to substitution of the alcoholic proton at the 2-position with a methyl group. This structure enhances the intermolecular hydrogen-bonding ability of the alcoholic -OH group at the 3-position with water. Substitution at the 2- and 6-positions in DM $\beta$ -CD also increases the hydrophobicity of the cavity,<sup>28,29</sup> which leads to a greater strength of association of BP(OH)<sub>2</sub> with DM $\beta$ -CD compared to that with  $\beta$ -CD and enhances more penetration of BP(OH)<sub>2</sub> inside the cavity of DM $\beta$ -CD. This is reflected in the dramatic decrease in the absorbance intensity in the region 400–450 nm for the BP(OH)<sub>2</sub>/DM $\beta$ -CD complex, as shown in Figure 2.

The spectra in Figure 2 show a region near 368 nm where intersections occur, but over the range of CDs concentrations studied, isosbestic points are not maintained. The existence of one or more isosbestic points in the steady state spectra usually implies the presence of a single equilibrium between two species or two states.<sup>30</sup> However, it is evident that a system might possess only two states yet fail to exhibit a sharp isosbestic point if a spectral solvent dependence is operative.<sup>31</sup> This is the case of BP(OH)<sub>2</sub> in which solvation by water results in a dramatic change in the absorption spectral features and the peaks in the region of 400–450 nm are only feasible in water.<sup>18,26,27</sup> We have recently analyzed the change in the absorbance of BP(OH)<sub>2</sub> in binary mixtures of 1,4-dioxane/water of different compositions and concluded that high water contents tend to solvate the two hydrogen bonding centers in BP(OH)<sub>2</sub>.<sup>18</sup> Accordingly, the absence of sharp isosbestic points in the absorption spectra in Figure 2 is not an indication of the formation of complexes higher than 1:1 between BP(OH)<sub>2</sub> and each of the CD hosts studied here, but the overall changes in the spectra are due to the caging effect of CDs on BP(OH)<sub>2</sub>.

**Determination of the Stoichiometric Ratios and Binding Constants.** The stoichiometric ratios and the binding constants

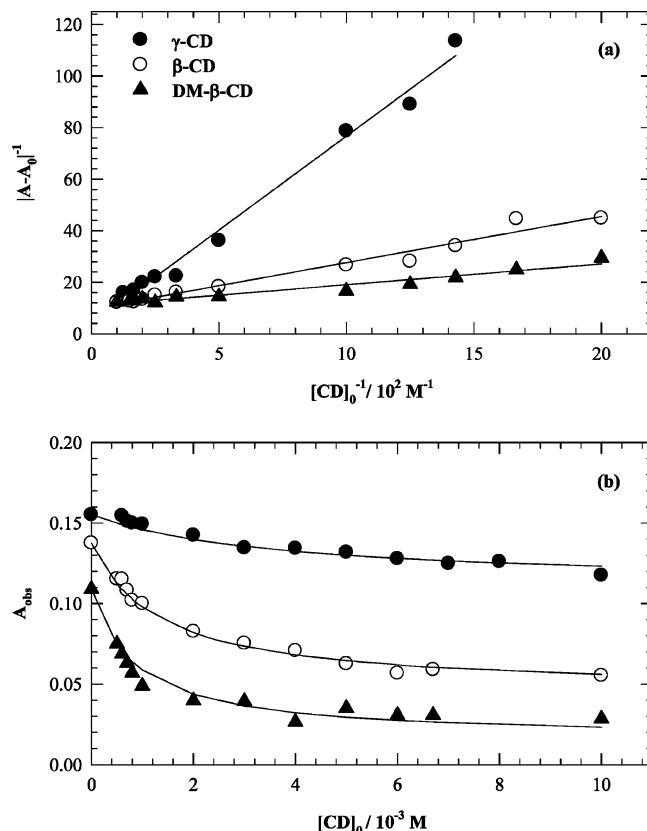


**Figure 4.** (a) BH double-reciprocal plots (eq 1) using absorbance data at 409 nm for the BP(OH)<sub>2</sub> molecule complexed with the three CD hosts, as indicated in the figure for  $n = 1$ . (b) Variation of absorbance intensity of the BP(OH)<sub>2</sub> molecule complexed with the three CD hosts at 409 nm as a function of [ $\gamma$ -CD], [ $\beta$ -CD] and [DM $\beta$ -CD], as indicated in the figure. The solid lines are the best NLR fits using eq 4 for  $n = 1$ .

of the complexes were estimated from the Benesi–Hildebrand (BH) double reciprocal plots,<sup>32</sup> which correlate the changes in the absorption intensities to the CDs' concentrations<sup>33,34</sup> according to

$$\frac{1}{|A - A_0|} = \frac{1}{(\epsilon_c - \epsilon_0)[N]_0} + \frac{1}{(\epsilon_c - \epsilon_0)[N]_0 K [CD]_0^n} \quad (1)$$

where  $A$  and  $A_0$  are the absorbances per centimeter of BP(OH)<sub>2</sub> aqueous solution in the presence and absence, respectively, of CD;  $\epsilon_c$  and  $\epsilon_0$  are the molar absorption coefficients of BP(OH)<sub>2</sub>/CD complex and BP(OH)<sub>2</sub>, respectively;  $[N]_0$  is the initial concentration of BP(OH)<sub>2</sub>;  $[CD]_0$  is the initial concentration of CD;  $n$  represents the stoichiometry of the equilibrium reaction in relation to CD; and  $K$  is the equilibrium constant for the formation of BP(OH)<sub>2</sub>/CD. Because the concentration of CD is much higher than that of BP(OH)<sub>2</sub>,  $[CD]_0$  is assumed constant before and after complexation.

Thus, a plot of  $|A - A_0|^{-1}$  vs  $[CD]^{-n}$  should yield a straight line for the correct stoichiometry ( $n$ ). Typical double reciprocal plots are shown in Figure 4a for BP(OH)<sub>2</sub>/ $\gamma$ -CD, BP(OH)<sub>2</sub>/ $\beta$ -CD and BP(OH)<sub>2</sub>/DM $\beta$ -CD complexes, respectively. The absorption change at 409 nm was used for all the complexes. The absorbance at this wavelength is very sensitive to the degree of encapsulation as mentioned above. As shown in the figure, a straight line is obtained for each case when  $n = 1$ . These results suggest that the stoichiometry of the BP(OH)<sub>2</sub>/CD complexes are dominated by 1:1 (BP(OH)<sub>2</sub>:CD).

**TABLE 1: Estimated Binding Constants ( $K$  ( $M^{-1}$ )) for  $BP(OH)_2$  in Different CDs**

CD data <sup>a</sup>	absorbance data <sup>a</sup>	fluorescence
$\gamma$ -CD	385 ( $\pm 100$ )	335 ( $\pm 80$ )
$\beta$ -CD	860 ( $\pm 95$ )	875 ( $\pm 85$ )
DM $\beta$ -CD	1170 ( $\pm 135$ )	1188 ( $\pm 100$ )

<sup>a</sup> Uncertainties are shown in parentheses.

The guest:CD complex formation may be represented by the following relationship:

$$\frac{[B(CD)_n]}{[B]} = K[CD]_0^n \quad (2)$$

where  $[B(CD)_n]$  represents the concentration of complexed guest molecules by CD molecules and  $[B]$  is the concentration of the uncomplexed guest molecules. The rest of the parameters have the same meanings as in eq 1. An expression relating the relative concentrations to the observed absorbance ( $A_{obs}$ ), and to the absorbances of the complexed ( $A_{B(CD)_n}$ ) and uncomplexed ( $A_B$ ) guest molecules is given by<sup>31</sup>

$$\frac{[B(CD)_n]}{[B]} = \frac{(A_{obs} - A_B)}{(A_{B(CD)_n} - A_{obs})} \quad (3)$$

Combining eqs 2 and 3, one obtains the expression

$$A_{obs} = \frac{A_B + KA_{B(CD)_n}[CD]_0^n}{1 + K[CD]_0^n} \quad (4)$$

Plots of  $A_{obs}$  vs  $[CD]_0$  are depicted in Figure 4b for the three complexes.

The equilibrium constant for each complex formation was estimated from the slope and intercept of the BH double reciprocal plots shown in Figure 4a and used as an initial guess in an iterative nonlinear regression (NLR) fit using eq 4. More accurate  $K$  values are usually obtained from NLR fits than those estimated from the double reciprocal plots.<sup>30,33,35</sup> The fits are displayed in Figure 4b, and the resulting  $K$  values are shown in Table 1 with their corresponding uncertainties. The best NLR fits in all three complexes were for  $n = 1$ , which confirm the dominant 1:1 complexes. The  $K$  values reflect the relative stabilities of the three complexes and follow the same trend as discussed earlier.

**Steady State Fluorescence Spectra.** The steady state fluorescence spectra of the three complexes studied here behave similarly with a few exceptions, which will be discussed below. The fluorescence spectra of the  $BP(OH)_2$ : $\beta$ -CD complex are shown in Figure 5 as an example for excitation at (a) 344 nm and (b) 409 nm. Fluorescence in  $BP(OH)_2$  is due to the DK tautomer after ESIDPT in the excited state.<sup>15,18</sup> Increasing the CD concentration leads to a red shift of the fluorescence peak resulting from excitation at 344 nm with an increase in the intensity. On the other hand, the fluorescence peak resulting from excitation at 409 nm shows a decrease in the intensity with no measurable shift. The change in intensity upon excitation at 344 and 409 nm is well-correlated with the change in the corresponding intensities in the absorption spectra as a function of  $[CD]$  (see Figure 2). The red shift in the fluorescence peak after excitation at 344 nm is due to a change in environment from high to low polarity.<sup>18</sup> The latter is experienced as a result of the caging effect of the CD cavity. The intensity decrease in the fluorescence peak after excitation at 409 nm confirms the

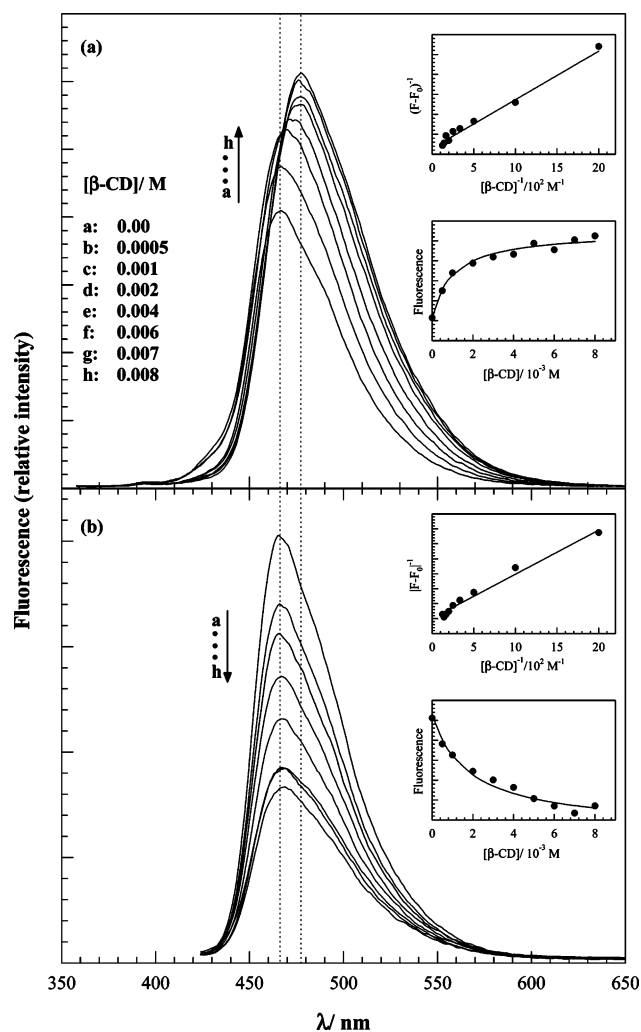


**Figure 5.** Fluorescence spectra of  $BP(OH)_2$  in aqueous solutions with varying concentrations of  $\beta$ -CD, as indicated in the figure after excitation at (a) 344 nm and (b) 409 nm. The insets show the same plots as in Figure 4 using the fluorescence intensities.

more hydrophobic environment experienced by the guest molecule as the CD concentration increases.

Excitation at the near isosbestic point (368 nm) results in spectra similar in their red shifts to those measured for excitation at 344 nm (data not shown). The intensities of the obtained spectra decrease in a manner similar to those measured for excitation at 409 nm. This observation implies the existence of an absorption overlap from the two peaks at 344 and 409 nm.

The normalized fluorescence spectra of  $BP(OH)_2$  in the three CDs studied here are depicted in Figure 6 after excitation at 344 nm. The spectra of  $BP(OH)_2$  in water and cyclohexane are also included for comparison. A red shift of ca. 36 nm in the fluorescence peak is observed by changing the solvent from strongly polar, protic water to nonpolar, aprotic cyclohexane. The fluorescence peaks in the host CDs lie between those in water and cyclohexane. This observation is a manifestation of the caging effect on the fluorescence of the DK tautomer.<sup>18</sup> As shown in Figure 6, the maximum shift is measured in the case of DM $\beta$ -CD, which confirms the more hydrophobic environment experienced by the guest molecule in this cavity (vide supra).

The results shown in Figure 6 may suggest a method to quantify the polarity of a given CD cavity by comparing the position of the fluorescence peak with that measured in different solvents. However, such a correlation is complicated for the present system by the fact that the fluorescence peak shift in

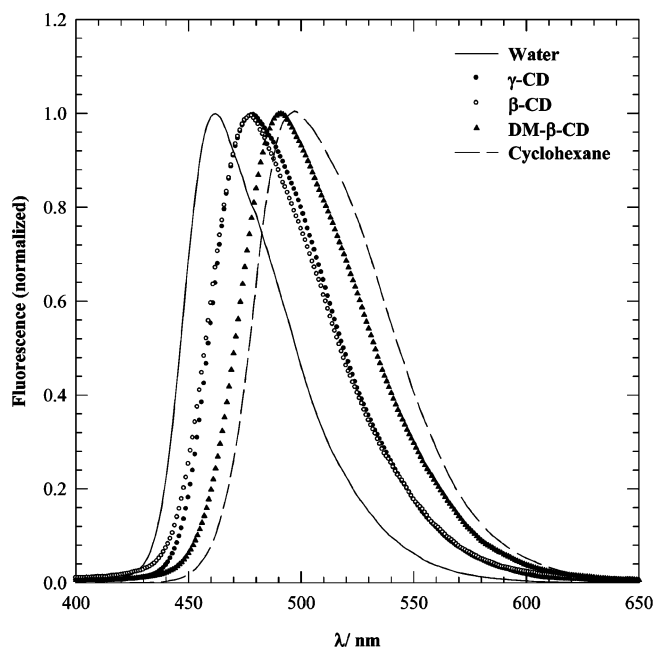


**Figure 6.** Fluorescence spectra of BP(OH)<sub>2</sub> in water, cyclohexane and in aqueous solutions of the three CD hosts, as indicated in the figure. The concentration of each host used was 0.01 M.

different solvents proved to be a function of not only the polarity of the solvent but also its hydrogen bonding capability.<sup>18</sup> For example, the fluorescence peak position was measured in methanol ( $\epsilon = 32.66$ ,  $\pi^* = 0.60$ )<sup>36</sup> at 476 nm, whereas in acetonitrile ( $\epsilon = 35.94$ ,  $\pi^* = 0.75$ )<sup>36</sup> it was measured at 493 nm. This observation contradicts the trend observed in Figure 6 if only polarity was accounted for. Because methanol is less polar than acetonitrile, the observed blue shift in methanol must derive from intermolecular hydrogen bonding interaction between BP(OH)<sub>2</sub> and methanol in the excited state potential energy surface as suggested by Marks et al.<sup>12</sup>

The binding constants for the three complexes were estimated from the fluorescence data. Equation 1 can be modified as<sup>30,33,35</sup>

$$\frac{1}{F - F_0} = \frac{1}{F_c - F_0} + \frac{1}{(F_c - F_0)K[\text{CD}]_0^n} \quad (5)$$

where  $F$  and  $F_0$  are the fluorescence intensities of BP(OH)<sub>2</sub> aqueous solution in the presence and absence, respectively, of CD; and  $F_c$  is the intensity due to the BP(OH)<sub>2</sub>/CD complex only. NLR fits to Equation 4 are also used by replacing the absorbance terms by the corresponding fluorescence terms. The fittings to Equations 4 and 5 are shown in Figure 5 for BP(OH)<sub>2</sub>/β-CD and the obtained equilibrium constants for the three complexes are included in Table 1. The values of  $K$ 's obtained by both absorbance and fluorescence data agree within experimental uncertainties.

Preliminary results for the caging effect of α-CD on BP(OH)<sub>2</sub> indicate the formation of 1:2 complexes (one guest:two hosts). The small cavity size of α-CD is expected to prevent the inclusion of the whole guest molecule in one α-CD cavity. It is difficult to correlate these results with the present study due to the different complex order. The study of the inclusion of BP(OH)<sub>2</sub> inside the α-CD cavity will be the subject of a separate paper.

**Structural Calculations.** The structure of BP(OH)<sub>2</sub>/β-CD was calculated using ab initio methods. The structural parameters known from the X-ray studies were used as a starting point for β-CD<sup>37</sup> and BP(OH)<sub>2</sub>.<sup>6</sup> The BP(OH)<sub>2</sub> (guest) molecule was then

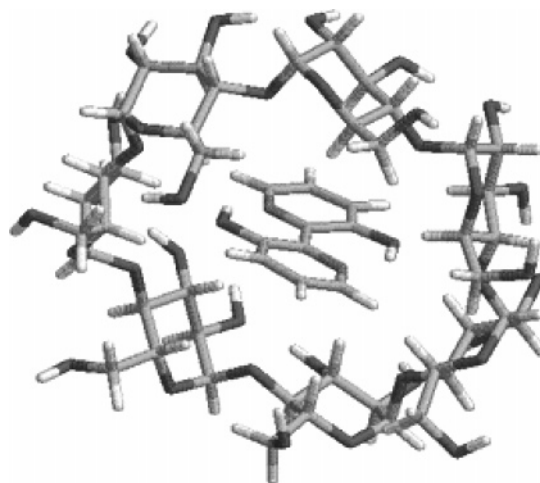


**Figure 7.** Structure of the most stable minimum configuration of BP(OH)<sub>2</sub> embedded inside the β-CD cavity. The structure is obtained from ab initio calculations described in the text. View is looking up through the secondary-hydroxy rim (wider opening) to the primary-hydroxy rim (narrower opening) of β-CD.

introduced inside the β-CD (host) cavity. The complex was allowed to optimize using a 3-21G basis set with no restrictions.

The minimum-energy confirmation found in the search is depicted in Figure 7. The final parameters for the β-CD molecule are not very different from the initial (X-ray) ones. On the other hand, the final structure of the guest molecule shows a small deviation of 5.1° between the planes of the two aromatic rings. The intramolecular O—H...N hydrogen bonds are not perturbed, as the interatomic distances between the three atoms in each hydrogen bonding center are not appreciably modified upon encapsulation.

The orientation of the guest molecule is axial inside the CD cavity with a tilt angle of 26° between the long axis of the guest and the axial axis of the CD molecule. The guest molecule is also completely sequestered in the center of the CD cavity. The BP(OH)<sub>2</sub> molecule stayed inside the cavity throughout the optimization, indicating that the energy of the complex is less than the sum of the energy of the separated host and guest molecules. Analysis of the host—guest interatomic distances shows that the closest H(host)—O(guest) distance is 2.2 Å, and the closest H(host)—N(guest) distance is 2.6 Å. This indicates that the moiety of the guest molecule remains isolated inside the cavity and intramolecularly hydrogen-bonded in the DE form.

**BP(OH)<sub>2</sub> as a Potential Biological Probe.** The spectral changes due to the caging effects of CDs reveal important features for BP(OH)<sub>2</sub> as a potential biological probe. The absorption peaks due to water solvation in the ground state (see Figure 3) may act as a probe of how BP(OH)<sub>2</sub> is shielded from water in solution. Because the two peaks at 409 and 435 nm are due to water complexes with BP(OH)<sub>2</sub>,<sup>18,26</sup> these peaks can be used as a probe of the accessibility of the BP(OH)<sub>2</sub> molecule to water. This is important in biological systems in which molecular probes are used to detect for example protein unfolding and DNA unwinding. Also, the progressive red shift in the fluorescence peak of the DK tautomer (Figure 6) and the change in its intensity (Figure 5) as a function of hydrophobicity of the CD cavities make BP(OH)<sub>2</sub> a unique probe in biological systems using fluorescence measurements. Studying the spectroscopy of BP(OH)<sub>2</sub> in biological systems is in progress in this laboratory.

## Conclusions

The inclusion of the BP(OH)<sub>2</sub> molecule inside the cavities of  $\gamma$ -CD,  $\beta$ -CD and DM $\beta$ -CD was studied using absorption and fluorescence spectroscopy, and by ab initio calculations. The changes in the absorption and fluorescence spectra of BP(OH)<sub>2</sub> as a function of varying the initial concentrations of CDs indicate different caging effects due to the change in the cavity size and hydrophobicity. In the case of  $\gamma$ -CD, the large cavity size supports only small binding, whereas such binding increases in the cases of the smaller cavity sizes of  $\beta$ -CD and DM $\beta$ -CD. In the latter, maximum binding was measured due to the increased hydrophobicity as a result of the methyl substituents. The stoichiometric ratio was deduced from fitting the changes in the spectral intensities to BH and NLR algorithms and was found to be 1:1 in all the complexes. Ab initio calculations of the BP(OH)<sub>2</sub>: $\beta$ -CD structure indicate that the inclusion of the guest molecule is axial and centered inside the host cavity. The BP(OH)<sub>2</sub> molecule maintains its DE moiety with no possible hydrogen bonding with the host interior H-atoms.

The caging effects on the absorption and fluorescence spectra of BP(OH)<sub>2</sub> following complexation with CDs suggest that this molecule can be used as a possible water sensor in biological systems.

**Acknowledgment.** This work was supported by the Sultan Qaboos University (grant no. IG/SCI/CHEM/05/03).

## References and Notes

- (1) Bulska, H. *Chem. Phys. Lett.* **1983**, *98*, 398.
- (2) Bulska, H.; Grabowska, A.; Grabowski, Z. R. *J. Lumin.* **1986**, *35*, 189.
- (3) Sepiol, J.; Bulska, H.; Grabowska, A. *Chem. Phys. Lett.* **1987**, *140*, 607.
- (4) Kaschke, M.; Rentsch, S.; Opfermann, J. *Laser Chem.* **1988**, *8*, 377.
- (5) Sepiol, J.; Grabowska, A.; Bulska, H.; Mordzinski, A.; Perez Salgado, F.; Rettschnick, R. P. H. *Chem. Phys. Lett.* **1989**, *163*, 443.
- (6) Lipkowski, J.; Grabowska, A.; Waluk, J.; Calestani, G.; Hess, B. A. *J. Crystallogr. Spectrosc. Res.* **1992**, *22*, 563.
- (7) Wortmann, R.; Elich, K.; Lebus, S.; Liptay, W.; Borowicz, P. *J. Phys. Chem.* **1992**, *96*, 9724.
- (8) Borowicz, P.; Grabowska, A.; Wortmann, R.; Liptay, W. *J. Lumin.* **1992**, *52*, 265.
- (9) Zhang, H.; van der Meulen, P.; Glasbeek, M. *Chem. Phys. Lett.* **1996**, *253*, 97.
- (10) Marks, D.; Proposito, P.; Zhang, H.; Glasbeek, M. *Chem. Phys. Lett.* **1998**, *289*, 535.
- (11) Proposito, P.; Marks, D.; Zhang, H.; Glasbeek, M. *J. Phys. Chem. A* **1998**, *102*, 8894.
- (12) Marks, D.; Zhang, H.; Glasbeek, M.; Borowicz, P.; Grabowska, A. *Chem. Phys. Lett.* **1997**, *275*, 370.
- (13) Toebe, P.; Zhang, H.; Glasbeek, M. *J. Phys. Chem. A* **2002**, *106*, 3651.
- (14) Barone, V.; Adamo, C. *Chem. Phys. Lett.* **1995**, *241*, 1.
- (15) Sobolewski, A. L.; Adamowicz, L. *Chem. Phys. Lett.* **1996**, *252*, 33.
- (16) Barone, V.; Palma, A.; Sanna, N. *Chem. Phys. Lett.* **2003**, *381*, 451.
- (17) Gelabert, R.; Moreno, M.; Lluch, J. M. *ChemPhysChem.* **2004**, *5*, 1372.
- (18) Abou-Zied, O. K. *J. Photochem. Photobiol. A*, in press.
- (19) Bender, M. L.; Komiyama, M. *Cyclodextrin Chemistry*; Springer: Berlin, 1978.
- (20) (a) D'Souza, V. T.; Bender, M. L. *Acc. Chem. Res.* **1987**, *20*, 146. (b) Szejtli, J. *Cyclodextrins and their Inclusion Complexes*; Budapest, 1982; p 25.
- (21) Ramamurthy, V. *Photochemistry in Organized and Constrained Media*; VCH: New York, 1991.
- (22) (a) Douhal, A. *Chem. Rev.* **2004**, *104*, 1955. (b) Li, S.; Purdy, W. C. *Chem. Rev.* **1992**, *92*, 1457.
- (23) Yorozu, T.; Hoshino, M.; Imamura, M.; Shizuka, H. *J. Phys. Chem.* **1982**, *86*, 4422.
- (24) Shizuka, H.; Fukushima, M.; Fujii, T.; Kobayashi, T.; Ohtani, H.; Hoshino, M. *Bull. Chem. Soc. Jpn.* **1985**, *58*, 2107.
- (25) Schmidt, M. W.; Baldrige, K. K.; Boatz, J. A.; Elbert, S. T.; Gordon, M. S.; Jensen, J. H.; Koseki, S.; Matsunaga, N.; Nguyen, K. A.; Su, S. J.; Windus, T. L.; Dupuis, M.; Montgomery, J. A. *J. Comput. Chem.* **1993**, *14*, 1347.
- (26) Carballeira, L.; Perez-Juste, I. *J. Mol. Struct. (THEOCHEM)* **1996**, *368*, 17.
- (27) Barone, V.; Palma, A.; Sanna, N. *Chem. Phys. Lett.* **2003**, *381*, 451.
- (28) Easton, C. J.; Lincoln, S. F. *Modified Cyclodextrins*; Imperial College Press: London, 1999.
- (29) Steiner, T.; Saenger, W. *Carbohydr. Res.* **1995**, *275*, 73.
- (30) Mwalupindi, A. G.; Rideau, A.; Agbaria, R. A.; Warner, I. M. *Talanta* **1994**, *41*, 599.
- (31) Connors, K. A. *Binding Constants. The Measurements of Molecular Complex Stability*; Wiley: New York, 1987.
- (32) Benesi, A. H.; Hildebrand, J. H. *J. Am. Chem. Soc.* **1949**, *71*, 2703.
- (33) Abou-Zied, O. K. *Spectrochim. Acta A* **2005**, *62*, 245.
- (34) Hamai, S. *Bull. Chem. Soc. Jpn.* **1982**, *55*, 2721.
- (35) (a) Mitra, S.; Das, R.; Mukherjee, S. *J. Phys. Chem. B* **1998**, *102*, 3730. (b) Roberts, E. L.; Dey, J.; Warner, I. M. *J. Phys. Chem.* **1996**, *100*, 19681.
- (36) Reichardt, C. *Solvents and Solvent Effects in Organic Chemistry*; VCH: Weinheim, 1988.
- (37) Betzel, C.; Saenger, W.; Hingerty, B. E.; Brown, G. M. *J. Am. Chem. Soc.* **1984**, *106*, 7545.